RSC Advances

This is an *Accepted Manuscript*, which has been through the Royal Society of Chemistry peer review process and has been accepted for publication.

Accepted Manuscripts are published online shortly after acceptance, before technical editing, formatting and proof reading. Using this free service, authors can make their results available to the community, in citable form, before we publish the edited article. This *Accepted Manuscript* will be replaced by the edited, formatted and paginated article as soon as this is available.

You can find more information about *Accepted Manuscripts* in the Information for Authors.

Please note that technical editing may introduce minor changes to the text and/or graphics, which may alter content. The journal's standard Terms & Conditions and the Ethical guidelines still apply. In no event shall the Royal Society of Chemistry be held responsible for any errors or omissions in this *Accepted Manuscript* or any consequences arising from the use of any information it contains.

ROYAL SOCIETY OF CHEMISTRY

www.rsc.org/advances

TOC

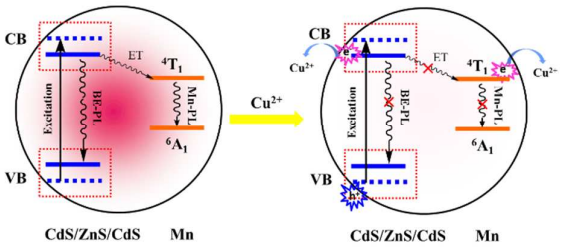

Energy levels of Mn-doped QD-based nanosensor and the quenching mechanism of the nanosensor by Cu^{2+}

RSC Advances Accepted Manuscript

Journal Name

RSCPublishing

ARTICLE

Mn-Doped CdS/ZnS/CdS QD-Based Fluorescent Nanosensor for Rapid, Selective, and Ultrasensitive Detection of Copper (II) Ion

Cite this: DOI: 10.1039/x0xx00000x

Received 00th January 2012,
Accepted 00th January 2012

DOI: 10.1039/x0xx00000x

www.rsc.org/

Xiaoman Zhai[a], Yunqian Gong[a], Wen Yang[a], Huaizhi Kang[b*], Xiaoling Zhang[a*]

A facile strategy for designing a glutathione-capped Mn-doped CdS/ZnS/CdS core/shell/shell QD-based fluorescent nanosensor has been developed for rapid, selective, and ultrasensitive detection of Cu^{2+}. In this nanosensor, glutathione provided the binding and recognition sites for Cu^{2+}, accumulating Cu^{2+} on the QD surface. The energy transfer pathway from the host to the Mn dopant was sensitive to the interferences from non-radiative recombination pathways caused by Cu^{2+}, resulting in photoluminescence quenching. The nanosensor responsed to Cu^{2+} within one minute and exhibited good selectivity to Cu^{2+} over other metal ions and good linear correlation over the concentration range of 1 nM to 100 nM, with a detection limit as low as 0.74 nM. Moreover, this nanosensor avoids the self-quenching problem and autofluorescence in biosystems due to the substantial Stokes shift and long lifetime, and thus can be used to monitor Cu^{2+} in living cells.

Introduction

Copper is an essential transition element in environmental or biological systems. As one of the most important trace elements, copper plays a pivotal role in a variety of fundamental physiological and pathological events for humans and other animals.[1] However, excess copper ions (Cu^{2+}) may become toxic to living organisms and bring health risks, such as Menkes, Wilson disease, and Alzheimer's disease.[2] Accordingly, the U.S. Environmental Protection Agency (EPA) has set a limit of 1.3 ppm or ~20 μM for Cu^{2+} levels in drinking water.[3] Thus, various techniques such as atomic absorption spectrometry, inductively coupled plasma mass spectroscopy (ICP-MS), inductively coupled plasma atomic emission spectrometry (ICP-AES), and fluorimetric spectrometry have been developed for Cu^{2+} determination.[4] In the past decade, designs of fluorescent biosensors for Cu^{2+} detection have attracted considerable attention, based on their simplicity, low cost, high sensitivity, and rapid analysis. Organic fluorophores were widely used as fluorescent Cu^{2+} sensors.[5] However, some drawbacks such as complicated organic synthesis and purification, cross-sensitivity toward other metal ions, or low quantum yields (QYs) restrict their practical applications. Moreover, DNAzyme-based sensors have also been developed for Cu^{2+} detection, but there are still some limiting factors such as high cost for preparing DNAzyme labelled with fluorophore.[3, 6] Therefore, the development of new Cu^{2+} fluorescent sensors which are sensitive, selective, biocompatible, and low cost is highly desirable.

As optical sensors, semiconductor quantum dots (QDs) exhibit a promising prospect because of their unique properties, such as broad absorption, size- and component-tunable emission, and high photoluminescence (PL) QYs.[7] These favourable optical properties and versatile surface modification permit construction of various QD-based PL sensing platforms.[8] The pioneering work by Chen and Rosenzweig showed great progress in detecting metal ions, in which luminescent CdS QDs were employed as an ion selective-sensor for Cu^{2+}, Zn^{2+} and Fe^{3+}.[9] Leblanc's group reported peptide-coated CdS QDs for Cu^{2+} and Fe^{3+} detection.[10] However, the cross-sensitivity toward other metal ions led to low selectivity. Isarov proposed a Cu^{2+} quenching mechanism involving formation of Cu_xS (x=1, 2) precipitate on the QD surface.[11] Although recent work has lowered the detection limit from micromolar to nanomolar levels, this type of sensor response to Cu^{2+} slowly.[12] Moreover, a major problem hampering QD applications in biosensing and bioimaging is the self-quenching caused by the small Stokes shift of the QDs or by energy transfer between adjacent QDs.[13]

Mn-doped QDs have been regarded as a promising new generation of fluorophores. Incorporation of Mn^{2+} into host lattices can yield materials with desirable properties and functions (e.g. large Stokes shift and long lifetimes). The substantial Stokes shift can effectively avoid the self-quenching problem mentioned above. Moreover, Mn-doped QDs exhibit long lifetimes, providing the opportunity to eliminate background fluorescence.[14] Thus, Mn-doped QDs are good candidates for constructing sensing platform.

In this work, Mn-doped CdS/ZnS/CdS core/shell/shell QD-based fluorescent nanosensor was developed for Cu^{2+} detection. To improve the efficiency of Mn emission and selectivity of nanosensor, an outer CdS shell was introduced, which can assist energy transfer from the host to the Mn dopant.[15] Glutathione (GSH) caps served as recognition and bonding sites for Cu^{2+} sites, thus accumulating Cu^{2+} on the QD surface, resulting in the high selectivity and rapid response. The ultrasensitive sensing principle was based on PL quenching of Mn^{2+} emission via Cu^{2+}-induced non-radiative recombination pathways, which blocked the energy transfer from the host to the Mn dopant. This nanosensor displayed the rapid, selective, and ultrasensitive detection of Cu^{2+} in aqueous solution with a detection limit as low as 0.74 nM. Due to the substantial

RSC Advances Accepted Manuscript

Stokes shift and long lifetime, the as-prepared nanosensor resolved the self-quenching problem and eliminated the background fluorescence so that it was also used to monitor Cu^{2+} in living cells.

Experimental

Materials and reagents

Sulphur powder (99.999%), 1-octanethiol (>98.5%), 1-octadecence (ODE, 90%), oleylamine (OAm, 70%), myristic acid (MA, 99%) 3-mercaptopropionic acid (MPA, tech. 99%), N-hydroxy succinimide (NHS, 98%), 1-(3-dimethylaminopropyl)-3-ethylcarbodiimide hydrochloride (EDC, 98%) and glutathione (GSH, 99%) were purchased from Sigma-Aldrich. Zinc stearate ($Zn(St)_2$, 14% ZnO%), cadmium oxide (CdO, 99.998%), cadmium nitride ($Cd(NO_3)_2$, 99.99%), and oleic acid (OA, 90%) were purchased from Alfa-Aesar. Manganese (II) acetate tetrahydrate ($Mn(OAc)_2{\cdot}4H_2O$, 98%), copper (II) nitrate trihydrate ($Cu(NO_3)_2{\cdot}3H_2O$, 99%), sodium hydroxide (NaOH, 99%), and all solvents were purchased from Beijing Chemical Reagents Cooperation. Chemicals were used as received without further purification. Phosphate buffer solution (PBS, 100 mM, pH=7.4) was prepared by mixing the solutions of K_2HPO_4 and NaH_2PO_4. Cadmium myristate ($Cd(myr)_2$) was prepared according to the literature method.[16] Dulbecco's modified Eagle's medium (DMEM) and fetal bovine serum (FBS) were purchased from Gibco (Beijing, China). Penicillin and streptomycin were purchased from Hyclone (Beijing, China). Nanopure water was used throughout all the experiments.

Stock solutions

Zinc stearate solution. 0.4 mmol $Zn(St)_2$ was added to a flask containing 10 mL of ODE. After degassing for 10 min at room temperature (RT), the mixture was heated to 200 °C to dissolve the zinc stearate. The solution was cooled to RT and a slurry formed. The slurry was directly used for ZnS shell growth.

Sulphur solution. 0.4 mmol S powder was added to a flask with 10 mL of ODE. After degassing for 10 min at RT, the solution was heated to 130 °C under Ar flow. The temperature was maintained for 5 min, and then the sulphur solution was cooled to RT for use.

Cadmium-Oleate solution. 0.2 mmol CdO powder was added to a flask with a mixture of OA (0.57 mL) and ODE (0.43 mL). After degassing at RT for 10 min and 60 °C for 10 min, the mixture was heated to 120 °C and kept for 10 min to dissolve CdO. After CdO was totally dissolved, 4 mL of ODE was injected into the flask to make the final precursor concentration 0.04 M.

1-octanethiol solution. 0.4 mmol 1-octanethiol was added into a flask with 10 mL of ODE. After degassing for 10 min at RT, the solution was heated to 130 °C under Ar flow. The temperature was maintained for 5 min, and then the 1-octanethiol solution was cooled to RT for use.

$Mn(OAc)_2$ solution. 4 mL of OAm was added into a 25 mL flask. After degassing for 10 min at RT, OAm solvent was heated at 120 °C for 10 min under a vacuum of 20 mTorr. After the OAm solvent was cooled to RT, $Mn(OAc)_2{\cdot}4H_2O$ (4.9 mg, 0.05 mM) was quickly added into the flask. The mixture was degassed at RT and at 120 °C for 10 min for each step. Then, the solution was cooled to RT. $Mn(OAc)_2$ solution should be freshly made before the synthesis.

Synthesis of Mn-doped CdS/ZnS/CdS QDs

The Mn-doped CdS/ZnS/CdS QDs were synthesized according to a modified method reported previously.[17] Briefly, CdS nanocrystals were first prepared using a non-injection synthesis.[16] 1 mmol $Cd(myr)_2$, 0.5 mmol S powder, and 50 g ODE were loaded into a three-neck round-bottom flask at RT. The resulting mixture was degassed at RT, and then was heated to 240°C under Ar flow. Serial aliquots were withdrawn to monitor the growth by UV-Vis spectroscopy. When the NCs reached the desired size, the reaction was stopped by rapidly cooling to RT. Then, the resulting CdS NCs were purified via precipitation by adding acetone. The suspension was centrifuged at 6,000 rpm for 10 min, the supernatant was discarded. The precipitates were redispersed in hexane and deposited by acetone. The above centrifugation and isolation procedure was then repeated three times for purification of CdS NCs. The final precipitates were redispersed in hexane as a high-concentration solution for further use.

Then, Mn-doped CdS/ZnS/CdS QDs were prepared according to successive ionic layer adsorption and reaction (SILAR).[18] A hexane solution of the CdS core (75 nmol) was added to a mixture solution of ODE and OAm (6.0 mL, ODE/OAm=1:1), and then hexane was removed under vacuum and the residue was flushed with argon. The flask was heated to 220 °C to grow the first two monolayers (MLs) of ZnS shell. The Zn precursor solution (0.63 mL) was firstly added via syringe to the flask. After 6 min, the same amount of S precursor solution was added, waiting 12 min to allow the growth of the first ZnS monolayer. Then, 0.87 mL of the Zn and S precursor solutions were injected alternately as before using the same time intervals. Then the growth temperature was raised to 280 °C and a $Mn(OAc)_2$ solution and sulphur solution (72 nmol, ($Mn(OAc)_2$ and sulphur at a molar ratio of 1:1) were alternatively introduced into the hot solution by dropwise addition. After 14 min, the third and fourth ML of ZnS shell were grown by adding the calculated amount of Zn and S precursor solutions (1.14 mL or 1.44 mL) of the precursor solutions to the reaction flask, respectively. After that the reaction solution was heated up to 310 °C. During the heating, 0.7 mL of Cd-oleate and octanethiol solutions were injected dropwise to the growth solution. After 20 min, the growth solution was cooled to RT. Then, the resulting QDs were isolated by adding acetone and further purified by three precipitation–redispersion cycles using ethanol and toluene. Finally, particles were dispersed in toluene.

Preparation of Water-Dispersible Mn-doped CdS/ZnS/CdS QDs

Ligand exchange was performed with MPA. To the Mn-doped CdS/ZnS/CdS QDs dispersed in 2 mL of toluene, 2 mL of MPA was added and stirred vigorously overnight at RT. Then, 400 μL of NaOH solution (0.05 M) was added to this solution and the mixture was centrifuged at 6,000 rpm·min^{-1} for 5 min. The centrifuged pellets were washed with chloroform three times.

Conjugation with GSH

The conjugation of MPA-stabilized Mn-doped CdS/ZnS/CdS QDs with GSH was achieved by EDC/NHS coupling. Typically, 8 mg of MPA-stabilized Mn-doped QDs were dispersed in 5 mL of PBS buffer. Then, 100 μL of EDC (0.05 M solution in PBS) and an equal amount of NHS (0.05 M solution in PBS) were added and stirred for 2 h.[19] Then, 100 μL of GSH (0.05 M solution in PBS) was added and stirred overnight. The unreacted materials were removed by dialysis against nanopure water using a 3.5-kD cut-off dialysis membrane.

Sensitivity and Selectivity Measurement

$Cu(NO_3)_2$ was used as the Cu^{2+} source for sensitivity and selectivity studies. A stock solution of $Cu(NO_3)_2$ (0.1 M) was prepared, and various concentrations were obtained by serial dilution of the stock solution. The detection of Cu^{2+} with different concentrations was performed in PBS buffer (10 mM, pH 7.4). The PL spectra were collected on a Hitachi F-7000 fluorescence spectrophotometer with excitation at 360 nm. Stock solutions of other metal ions (Na^+, K^+, Ca^{2+}, Ba^{2+}, Fe^{3+}, Mg^{2+}, Al^{3+}, Hg^{2+}, Co^{2+}, Cd^{2+}, Ni^{2+}, Pb^{2+}, Mn^{2+}, Zn^{2+}, and Ag^+) were prepared for the evaluation of the selectivity of the nanosensor.

RSC Advances Accepted Manuscript

 This journal is © The Royal Society of Chemistry 2012

Cell Culture and Confocal Imaging

HeLa cells were cultured in DMEM supplemented with 10% FBS and 1% penicillin/streptomycin. When in proliferative period, HeLa cells were seeded in glass bottom culture dishes and 1.5 mL culture medium was added. The dishes were then placed in an incubator at 37 °C with 5% CO_2 atmosphere for 24 h. After removal of the culture medium, cells were incubated with GSH-capped Mn-doped CdS/ZnS/CdS QD-based nanosensor in 1.5 mL of fresh culture medium (0.05 mg/mL). After 1 h of incubation, the dishes were rinsed five times with PBS to remove the residual QDs, and then 1.5 mL of culture medium was added. The dishes were incubated for another 10 min, and then washed with PBS five times. The cells were suspended in 2 mL of PBS and observed under an Olympus FV1000 laser confocal microscope. Both emissions from the GSH-capped Mn-doped QD-based nanosensor were excited at 405 nm and collected in the blue (415-450 nm) and red (550-650 nm) channels.

Results and discussion

Synthesis and characterization of GSH-capped Mn-doped CdS/ZnS/CdS QD-based fluorescent nanosensor

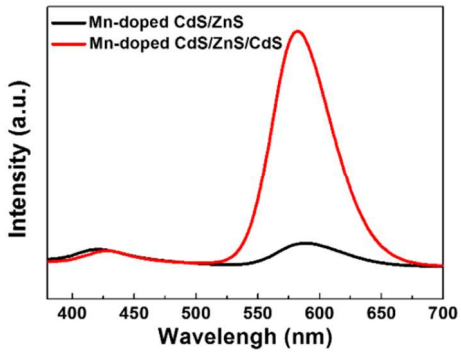

Fig. 1 PL spectra of Mn-doped QDs before and after growing outer CdS shell.

The Mn-doped CdS/ZnS/CdS QDs were prepared via a radial-position-controlled doping strategy. In order to improve the efficiency of the Mn emission, the outer CdS shell was introduced. Fig. 1 shows the PL spectra of QDs before and after growing the outer CdS shell. A substantial increase of the intensity of the Mn emission occurs, because the CdS shell not only removes the surface trap of Mn-doped QDs, but also facilitates the energy transfer from the host to the Mn dopant.[15, 20] The GSH-capped Mn-doped QD-based nanosensor used in this work was prepared through two steps, shown in scheme 1. First, water-soluble QDs can be obtained by ligand exchange with MPA. Second, the GSH-capped QDs were synthesized by the well-known EDC/NHS coupling to conjugate MPA-stabilized Mn-doped QDs with GSH in pH 7.4 PBS buffer. Typical TEM image of Mn-doped QDs are shown in Fig. 2A, exhibiting good monodispersity and high crystallinity. Fig. 2B shows the TEM image of GSH-capped Mn-doped QD-based nanosensor. The QDs in Fig. 2B are closer together than in Fig. 2A, because the ligand length of MPA is shorter than OAm, and the high ionic strength causes interparticle crosslinking of the QDs. Fig. 2C shows the UV-Vis and PL spectra of the as-prepared Mn-doped QDs in toluene and GSH-capped Mn-doped QD-based nanosensor in water. The absorption and PL peaks were located at 431 and 581 nm. The as-prepared Mn-doped QDs exhibited a large Stokes shift (ca. 150 nm), which resolved the self-quenching problem in biosensing and bioimaging. The absoption and PL peaks did not shift after replacing the long hydrophobic alkyl amine chains with the hydrophilic carboxyl chain of MPA. The emission peak at 581 nm, the characteristic dopant emission of Mn, can be assigned to the internal electronic transition of Mn^{2+} from $^4T_1$ to $^6A_1$.

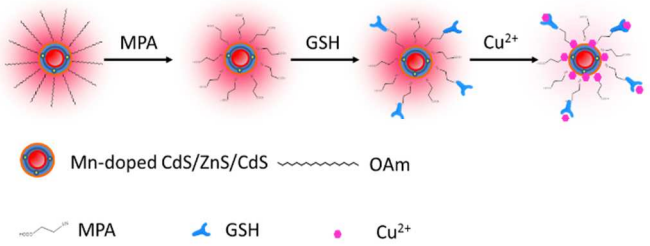

Scheme 1 Formation of GSH-capped Mn-doped CdS/ZnS/CdS QD-based fluorescent nanosensor for Cu^{2+}.

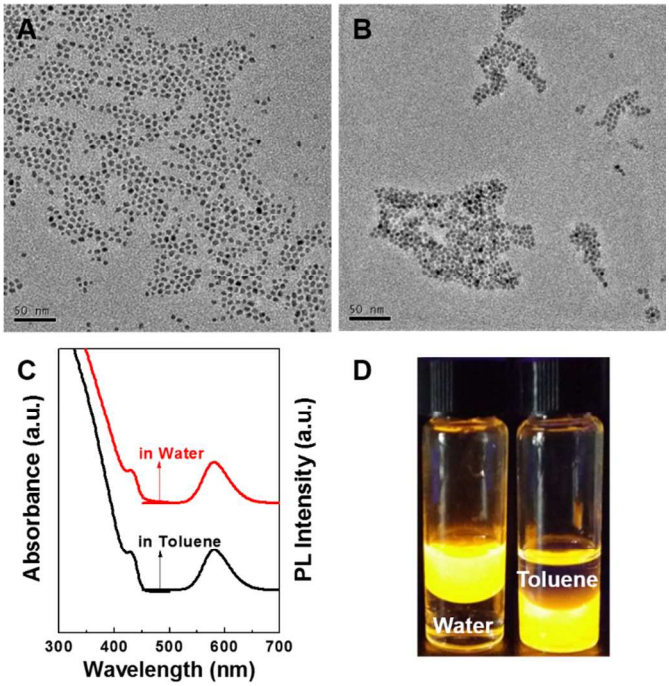

Fig. 2 TEM image of (A) Mn-doped CdS/ZnS/CdS QDs and (B) GSH-capped Mn-doped CdS/ZnS/CdS QD-based nanosensor. (C) Normalized UV-Vis absorption and PL spectra of Mn-doped CdS/ZnS/CdS QDs (in toluene, black lines) and GSH-capped Mn-doped CdS/ZnS/CdS QD-based nanosensor (in water, red lines). Excitation wavelength was 360 nm. (D) Digital pictures of the Mn-doped CdS/ZnS/CdS QDs before (left) and after (right) ligand exchange by irradiation with 365 nm light from a UV lamp.

Rapid and ultrasensitive detection of Cu^{2+}

The GSH-capped Mn-doped CdS/ZnS/CdS QD-based fluorescent nanosensor showed high sensitivity to Cu^{2+} in aqueous media. The detection strategy is illustrated in scheme 1. In the absence of Cu^{2+}, the Mn^{2+} emission is centred at 581 nm. Compared with the band-edge emission, the Mn^{2+} emission is more susceptible to interference by various non-radiative effects, which can be induced by Cu^{2+}. Thus, the Mn^{2+} emission is highly sensitive to Cu^{2+} and the PL intensity is gradually quenched as the concentration of Cu^{2+} increase. PL titration experiments were performed to evaluate the sensitivity of the GSH-capped Mn-doped QD-based fluorescent nanosensor toward Cu^{2+} as illustrated in Fig. 3A. Different concentrations of Cu^{2+} in the range of 0-20 μM were investigated. The inset of Fig. 3A shows the plot of I_0/I versus the concentration of Cu^{2+}, where I_0 and I are PL intensity at 581 nm in the absence and presence of Cu^{2+}, respectively. The relationship is described by the Stern-Volmer equation: $I_0/I=1+K_{sv}[Q]$, where [Q] is the concentration of Cu^{2+}, and

RSC Advances Accepted Manuscript

K_{sv} is the Stern-Volmer constant. At high concentration of Cu^{2+} (>500 nM), the PL intensity is very low, due to the saturation of the chelating sites by Cu^{2+} binding. Fig. 3B shows a good linear relationship (R^2=0.995) of (I_0/I) versus the concentration of Cu^{2+} over the range from 0 to 100 nM, and K_{sv} for Cu^{2+} was determined to be 0.018 nM^{-1}. The detection limit is as low as 0.74 nM. According to the data, over 90% of the PL intensity of Mn-doped QDs was quenched when the concentration of Cu^{2+} was 500 nM, and 97% PL was quenched when the concentration of Cu^{2+} reached 20 μM. To evaluate the response rate of the nanosensor to Cu^{2+}, time-dependent PL changes upon the addition of 500 nM Cu^{2+} were evaluated. As shown in Fig. 4, substantial PL quenching of Mn-doped QDs was observed within 1 min of contact time, indicating that the process of the non-radiative deactivation of Mn emission affected by Cu^{2+} is very rapid.

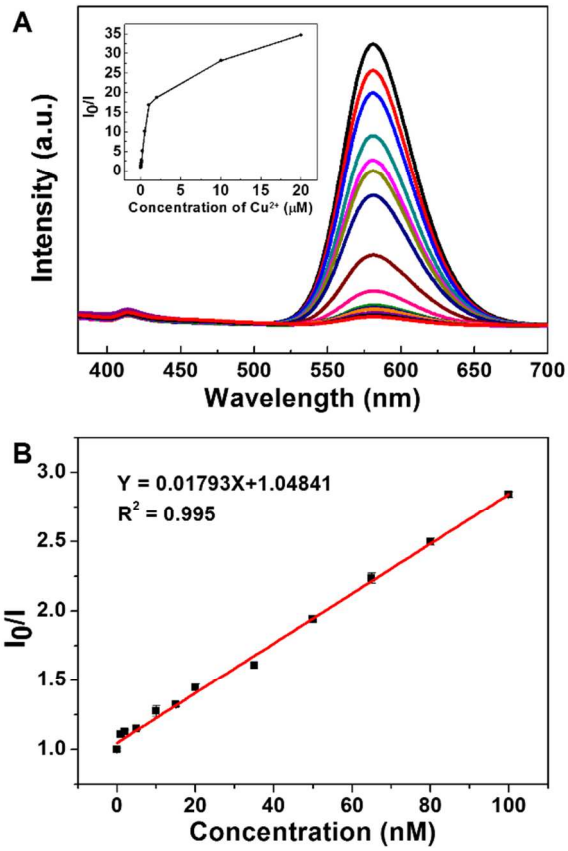

Fig. 3 (A) PL spectra of Mn-doped CdS/ZnS/CdS QD-based nanosensor after adding various concentrations of Cu^{2+} (from top to bottom: 0, 1×10^{-3}, 2×10^{-3}, 5×10^{-3}, 1×10^{-2}, 2×10^{-2}, 3.5×10^{-2}, 5×10^{-2}, 6.5×10^{-2}, 8×10^{-2}, 0.1, 0.2, 0.5, 1, 2, 10, and 20 μM). Inset: plots of PL intensity ratio (I_0/I) versus a different concentration of Cu^{2+}. (B) Linear fitting curve of PL intensity ratio (I_0/I) versus concentration of Cu^{2+}.

Selectivity and specificity of the nanosensor

Besides sensitivity, selectivity is also crucial to evaluate the performance of the nanosensor. Hence, we measured the PL response of the nanosensor in the presence of various metal ions. It can be seen that only Cu^{2+} caused dramatic fluorescence quenching (Fig. 5A), which suggests the good selectivity of the nanosensor to Cu^{2+} over other metal ions. In order to further investigate the sensing performance of this sensing system, an interference study was performed to verify that our nanosensor was not disturbed by other coexisting ions. In Fig. 5B, the response of the sensor to Cu^{2+} was almost unchanged, indicating that the coexistence of these metal ions had negligible interference on the detection of Cu^{2+}. In a word, the above results prove that our nanosensor exhibits high selectivity and specificity toward Cu^{2+}.

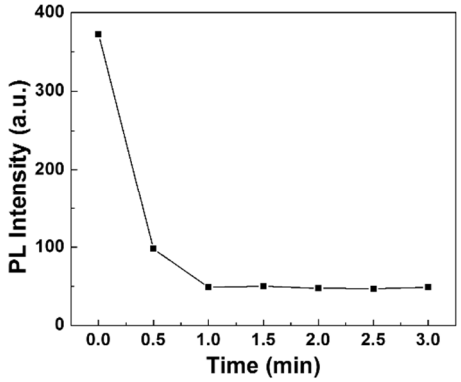

Fig. 4 PL quenching of Mn-doped CdS/ZnS/CdS QD-based nanosensor by 500 nM Cu^{2+} as a function of time. All solutions were prepared in PBS buffer (10 mM, pH 7.4).

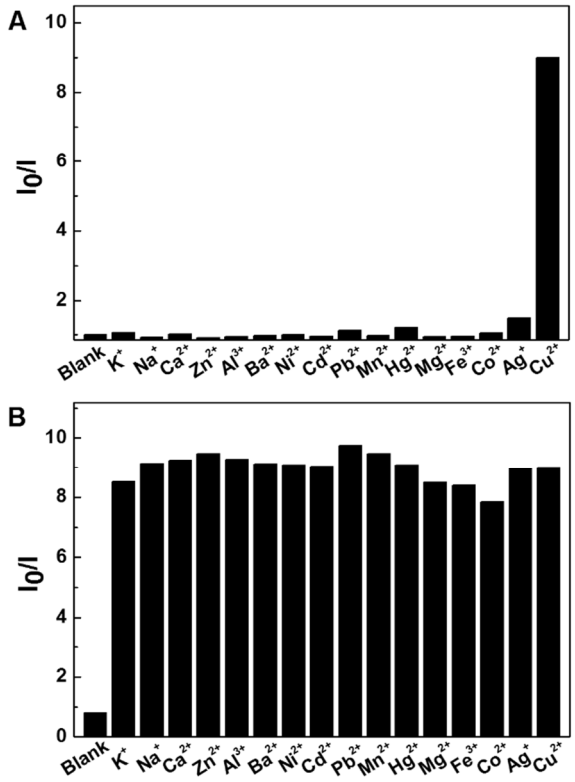

Fig. 5 (A) Selectivity of Mn-doped QD-based nanosensor toward various metal ions (the concentrations of the detected cations were all 500 nM). (B) Photoluminescence responses of Mn-doped QD-based nanosensor toward the interference of 500 nM of other metal ions with 500 nM Cu^{2+}. All solutions were prepared in PBS buffer (10 mM pH 7.4).

The probable mechanism

The possible mechanism for rapid, selective, and ultrasensitive detection of Cu^{2+} by the GSH-capped Mn-doped CdS/ZnS/CdS QD-based fluorescent nanosenor can be inferred from two considerations. Regarding selectivity, an important factor is the high intrinsic affinity between metal ion and the surface ligand.[19] In our nanosensor, GSH-capped Mn-doped QDs have

RSC Advances Accepted Manuscript

This journal is © The Royal Society of Chemistry 2012

a high affinity with Cu^{2+}, so that the possibility of direct interaction of the other metal ions with the QDs (non-specific interaction) is minimized, thus improving the selectivity. Furthermore, the interaction between GSH and Cu^{2+} allows Cu^{2+} to accumulate on the surface of the QDs for effective quenching of the QD PL. Scheme 2 shows the energy levels of the Mn-doped QD-based nanosensor and the quenching mechanism.[13, 21, 22] When a photon is absorbed by a Mn-doped CdS/ZnS/CdS QD, an electron-hole pair (an exciton) was created and confined inside the QD. The exciton can be deactivated by rapid energy transfer to Mn^{2+}.[14] As described by ligand-field theory, the ground state of Mn^{2+} is $^6A_1$ and the first excited state is $^4T_1$. After the energy is transferred to the Mn dopant, the excited Mn^{2+} relaxes from $^4T_1$ to $^6A_1$. The introduction of Cu^{2+} induces a non-radiative recombination of excited electrons in the conduction band and holes in the valence band of the host, thus blocking the energy transfer pathway from the QDs to Mn dopant.[21] In addition, Cu^{2+} can block the Mn^{2+} emission from $^4T_1$ to $^6A_1$ via non-radiative recombination as well. The energy of the electrons is released in non-radiative form, resulting in the quenching of PL.

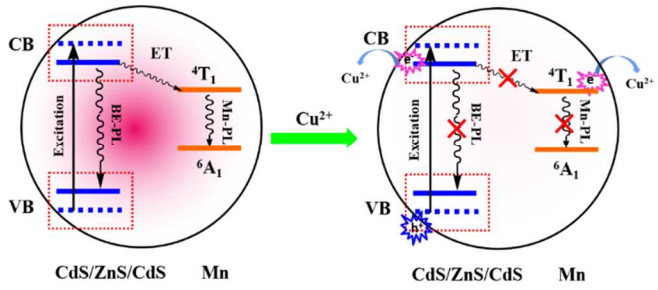

Scheme 2 Energy levels of Mn-doped QD-based nanosensor and the quenching mechanism of Mn-doped QD-based nanosensor by Cu^{2+}.

Fluorescence imaging of intracellular Cu^{2+}

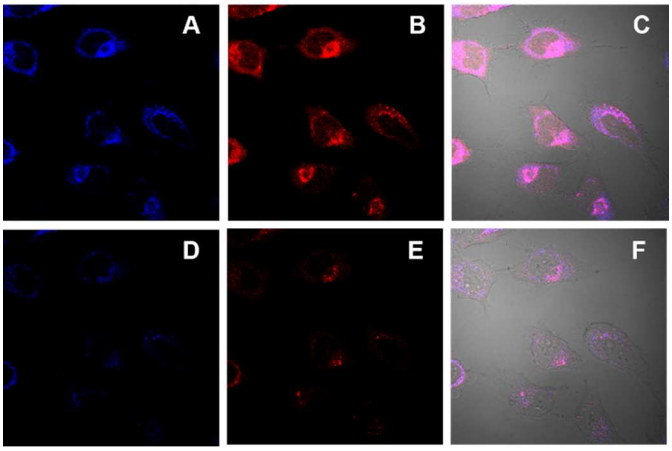

Fig. 6 Confocal fluorescent images of HeLa cells before (top) and after (bottom) addition of Cu^{2+} (20 μM). (A, D) Fluorescence images from blue channel (415-450 nm), (B, E) from the red channel (550-650 nm), and (C, F) overlay of fluorescence images and bright field images.

The Mn-doped QD-based nanosensor exhibited outstanding advantages such as sensitivity, selectivity and rapid response to Cu^{2+}. This nanosensor can also avoid the interference by autofluorescence of the biosystems. Therefore, the nanosensor was applied for monitoring Cu^{2+} in HeLa cells.[23] HeLa cells were incubated with the nanosensor for 1 h and then washed with PBS buffer five times. The fluorescence images of the blue (415-450 nm) and red (550-650 nm) channels were obtained with excitation by a 405 nm laser. As seen in Fig. 6, all the cells exhibited the clear cell morphology and strong fluorescences in the two channels. Compared with the fluorescence of the blue channel, the fluorescence of the red channel was much stronger, which is due to the high intensity of the Mn^{2+} emission. After addition of Cu^{2+} to HeLa cells, the fluorescence intensity of both channels decreased, but the fluorescence intensity of the red channel dropped rapidly. These results indicate that this nanosensor can be applied for monitoring Cu^{2+} in living cells.

Conclusions

In summary, a GSH-capped Mn-doped CdS/ZnS/CdS core/shell/shell QDs has been designed, synthesized and utilized as a highly efficient nanosensor for rapid, selective, and ultrasensitive Cu^{2+} detection. Cu^{2+}-induced non-radiative recombination blocks the energy transfer pathway from the QDs to Mn dopant, resulting in the quenching of Mn^{2+} emission. The limit of detection is as low as 0.74 nM. The nanosensor demonstrates excellent selectivity to Cu^{2+} over other metal ions. Moreover, the nanosensor can be further applied for monitoring Cu^{2+} in living cells.

Acknowledgements

We gratefully acknowledge financial support from the National Nature Science Foundation of China (No. 21275018 and 21203008), Research Fund for the Doctoral Program of Higher Education of China (RFDP) (No. 20121101110049) and the 111 Project (B07012) for financial support.

Notes and references

[a] Key Laboratory of Cluster Science of Ministry of Education, Beijing Key Laboratory of Photoelectronic/Electrophotonic Conversion Materials, School of Chemistry, Beijing Institute of Technology, Beijing 100081, P. R. China.
[b] College of Chemistry and Chemical Engineering, Xiamen University, Xiamen, Fujian 361005, P. R. China.
* Corresponding authors: Tel.: Fax: +86 1088 875298. E-mail address: zhangxl@bit.edu.cn (Xiaoling Zhang); kang@xmu.edu.cn (Huaizhi Kang).

1 (*a*) I. A. Koval, P. Gamez, C. Belle, K. Selmeczi and J. Reedijk, *Chem. Soc. Rev.*, 2006, **35**, 814; (*b*) Y. Fu, C.Q. Ding, A.W. Zhu, Z.F. Deng, Y. Tian and M. Jin, *Anal. Chem.*, 2013. **85**, 11936.
2 (*a*) B. Beauvoit, S. Evans, M. Jenkins, T. W. Miller and B. Chance, *Anal. Biochem.*, 1995, **226**, 167; (*b*) D.G. Barceloux, *J. Toxicol. Clin. Toxical.*, 1999, **37**, 217; (*c*) K. Welsher, Z. Liu, S. P. Sherlock, J. T. Robinson, Z. Chen, D. Daranciang and H. Dai, *Nat. Nanotechnol.*, 2009, **4**, 773; (*d*) K. J. Barnham, C. L. Masters and A. I. Bus, *Nat. Rev. Drug Discovery*, 2004, **3**, 205; (*e*) Q. Qu, A. W. Zhu, X. L. Shao, G. Y. Shi, Y. Tian, *Chem. Commun.*, 2012, **48**, 5473.
3 J. Liu and Y. Lu, *J. Am. Chem. Soc.*, 2007, **129**, 9838.
4 (*a*) T. W. Lin and S.D. Huang, *Anal. Chem.*, 2001, **73**, 4319; (*b*) T. Matoušek, A. Hernández-Zavala, M. Svoboda, L. Langrová, B. M. Adair, Z. Drobná, D. J. Thomas, M. Stýblo and J. Dědina, *Spectrochimica Acta Part B*, 2008, **63**, 396; (*c*) J. Djedjibegovic, T. Larssen, A. Skrbo, A. Marjanovic and M. Sober, *Food Chem.*, 2012, **131**, 469; (*d*) J. S. Becker, A. Matusch, C. Depboylu, J. Dobrowolska and M. V. Zoriy, *Anal. Chem.*, 2007, **79**, 6074; (*e*) G. H. Tao and R.

RSC Advances Accepted Manuscript

E. Sturgeon, *Spectrochimica Acta Part B*, 1999, **54**, 481; (*f*) Y. Liu, P. Liang and L. Guo, *Talanta*, 2005, **68**, 25; (*g*) Y. J. Zheng, J. Orbulescu, X. J. Ji, F. M. Andreopoulos, S. M. Pham and R. M. Leblanc, *J. Am. Chem. Soc.*, 2003, **125**, 2680; (*h*) Y. M. Guo, L. F. Zhang, S. S. Zhang, Y. Yang, X. H. Chen and M. C. Zhang, *Biosens. Bioelectron.*, 2014, **63**, 61.

5 (*a*) Q. Y. Wu and E. V. Anslyn, *J. Am. Chem. Soc.*, 2004, **126**, 14682; (*b*) M. Royzen, Z. Dai and J. W. Canary, *J. Am. Chem. Soc.*, 2005, **127**, 1612; (*c*) L. Zeng, E. W. Miller, A. Pralle, E. Y. Isacoff and C. J. Chang, *J. Am. Chem. Soc.*, 2005, **126**, 10; (*d*) W. C. Lin, C. Y. Wu and Z. H. Liu, Talanta, 2010, **8**, 1209; (*e*) K. P. Carter, A. M. Young and A. E. Palmer, *Chem. Rev.*, 2014, **114**, 4564.

6 (*a*) H. H. Yin, H. Kuang, L. Q. Liu, L. G. Xu, W. Ma, L. B. Wang and C. L. Xu, *ACS Appl. Mater. Interfaces*, 2014, **6**, 4752; (*b*) J. L. He, S. L. Zhu, P. Wu, P. P. Li, T. Li and Z. Cao, *Biosens. Bioelectron.*, 2014, **60**, 112.

7 (*a*) A. P. Alivisatos, *Science*, 1996, **271**, 933; (*b*) M. Bruchez Jr, M. Moronne, P. Gin, S. Weiss and A. P. Alivisatos, *Science*, 1998, **281**, 2013; (*c*) X. G. Peng, L. Manna, W. D. Yang, J. Wickham, E. Scher, A. Kadavanich and A. P. Alivisatos, *Nature*, 2000, **404**, 59; (*d*) Z. Pavel, S. Mark and X. Gao, *Chem. Soc. Rev.*, 2010, **39**, 4326.

8 (*a*) G. F. Jie, L. Wang, J. X. Yuan and S. S. Zhang, *Anal. Chem.*, 2011, **83**, 3873; (*b*) M. S. Wu, G. S. Qian, J. J. Xu and H. Y. Chen, *Anal. Chem.*, 2012, **84**, 5407; (*c*) H. H. Chen, Y. P. Ho, X. Jiang, H. Q. Mao, T. H. Wang and K. W. Leong, *Nano Today*, 2009, **4**, 125.

9 Y. Chen and Z. Roenzweig, *Anal. Chem.*, 2002, **74**, 5132.

10 K. M. Gattás-Asfura and R. M. Leblanc, *Chem. Commun.*, 2003, 2684.

11 A.V. Isarov and J. Chrysochoos, *Langmuir*, 1997, **13**, 3142.

12 Y. Q. Hao, L. Liu, Y. F. Long, J. X. Wang, Y. N. Liu, F. M. Zhou, *Biosens. Bioelectron.*, 2013, **41**, 723.

13 P. Wu and X. P. Yan, *Chem. Soc. Rev.*, 2013, **42**, 5489.

14 O. Chen, D. E. Shelby, Y. A. Yang, J. Q. Zhuang, T. Wang, C. G. Niu, N. Omenetto, Y. C. Cao, *Angew. Chem. Int. Ed.*, 2010, **49**, 10132.

15 S. Maiti, H. Y. Chen, Y. Park and D. H. Son, *J. Phys. Chem. C* , 2014, **118**, 18226.

16 Y. C. Cao and J. H. Wang, *J. Am. Chem. Soc.*, 2004, **126**, 14336.

17 (*a*) Y. A. Yang, O. Chen, A. Angerhofer and Y. C. Cao, *J. Am. Chem. Soc.*, 2006, **128**, 12428; (*b*) Y. A. Yang, O. Chen, A. Angerhofer and Y. C. Cao, *J. Am. Chem. Soc.*, 2008, **130**, 15649.

18 (*a*) J. J. Li, Y. A. Wang, W. Z. Guo, J. C. Keay, T. D. Mishima, M. B. Johnson and X. G. Peng, *J. Am. Chem. Soc.*, 2003, **125**, 12567; (*b*) B. Mahler, N. Lequeux and B. Dubertret, *J. Am. Chem. Soc.*, 2010, **132**, 953; (*c*) O. Chen, J. Zhao, V. P. Chauhan, Y. Cui, Y; C. Wong, D. K. Harris, H. Wei, H. S. Han, D. Fukumura, R. K. Jain and M. G. Bawendi, *Nat. Mater.*, 2013, **12**, 445; (*d*) D. A. Chen, F. Zhao, H. Qi, M. Rutherford and X. G. Peng, *Chem. Mater.*, 2010, **22**, 1437.

19 Y. Liu, T. Chen, C. C. Wu, L. P. Qiu, R. Hu, J. Li, Sena Cansiz, L. Q. Zhang, C. Cui, G. Z. Zhu, M. X. You, T. Zhang and W. H. Tan, *J. Am. Chem. Soc.*, 2014, **136**, 12552.

20 Y. A. Yang, O. Chen, A. Angerhofer and Y. C. Cao, *Chem. Eur. J.*, 2009, **15**, 3186.

21 Y. B. Lou, Y. X. Zhao, J. X. Chen and J. J. Zhu, *J. Mater. Chem. C*, 2014, **2**, 595.

22 P. Wu, T. Zhao, S. L. Wang, X. D. Hou, *Nanoscale*, 2014, **6**, 43.

23 M. Li, C. Y. Xu, L. Wu, P. Wu, X. D. Hou, *Chem. Commn*, 2015, **51**, 3552.

RSC Advances Accepted Manuscript

 This journal is © The Royal Society of Chemistry 2012